FEBRUARY 01 1997

Free vibration of a partially fluid-filled cross-ply laminated composite circular cylindrical shell

Z. C. Xi; L. H. Yam; T. P. Leung

J. Acoust. Soc. Am. 101, 909–917 (1997)
https://doi.org/10.1121/1.418049

Free vibration of a partially fluid-filled cross-ply laminated composite circular cylindrical shell

Z. C. Xi, L. H. Yam, and T. P. Leung
Department of Mechanical Engineering, The Hong Kong Polytechnic University, Hung Hom, Kowloon, Hong Kong

(Received 29 January 1996; accepted for publication 26 September 1996)

Free vibration of a partially fluid-filled cross-ply laminated composite circular cylindrical shell is investigated using a semi-analytical procedure based on the Reissner–Mindlin theory and compressible fluid equations. The shell is modeled using unaxisymmetric shear deformable circular cylindrical shell elements. The fluid is modeled using column fluid elements. The equation of motion of the partially fluid-filled shell is derived using the Hamilton's variational principle. Numerical examples are given for free vibrations of partially fluid-filled orthotropic and cross-ply laminated composite circular cylindrical shells with various boundary conditions. Numerical results indicate that the fluid filling can reduce significantly the natural frequencies of orthotropic and cross-ply laminated composite circular cylindrical shells. © *1997 Acoustical Society of America.* [S0001-4966(97)02502-2]

PACS numbers: 43.40.Ey, 43.20.Tb [CBB]

LIST OF SYMBOLS

$A_{ij}(i,j=1,2,6)$	extensional stiffness coefficients of the laminated composite shell
$A_{ij}(i,j=4,5)$	transverse shear stiffness coefficients of the laminated composite shell
$B_{ij}(i,j=1,2,6)$	extensional-bending coupling stiffness coefficients of the laminated composite shell
$D_{ij}(i,j=1,2,6)$	bending stiffness coefficients for the laminated composite shell
E	Young's modulus of isotropic material
E_1, E_2	Young's moduli of unidirectional composite in the 1 and 2 directions
G	shear modulus of isotropic material
G_{12}, G_{23}, G_{13}	shear moduli of unidirectional composite in the 1–2, 2–3, and 1–3 planes
h	thickness of the shell wall
H	height of the fluid
l	length of the shell element
L	length of the shell
m	axial half wave number
M_x, M_θ, $M_{x\theta}$	moment resultants
n	circumferential wave number
N_i, N_j	shape functions of the shell element
N_x, N_θ, $N_{x\theta}$	membrane stress resultants
P	hydrodynamic pressure
$Q_{\theta z}$, Q_{xz}	transverse shear stress resultants
$Q_{ij}(i,j=1,2,4,5,6)$	reduced stiffness coefficients of unidirectional composite
r	radial coordinate for the fluid
R	average radius of the shell
Rc	fundamental natural frequency ratio
u,v,w	middle surface displacements in axial, circumferential, and radial directions
$\dot{u},\dot{v},\dot{w}$	middle surface velocities in axial, circumferential, and radial directions
x	axial coordinate
z	radial coordinate for the shell
β_x, β_θ	rotations of the normal to the middle surface in the x and θ axes
$\gamma_{\theta z}$, γ_{xz}	transverse shear strains
δ_1, δ_2	defined by Eq. (29)
ε_x, ε_θ, $\varepsilon_{x\theta}$	middle surface strains
θ	circumferential coordinate
ζ	$\zeta=r/R$
η	$\eta=x/l$
ν	Poisson's ratio of isotropic material
ν_{12}	Poisson's ratio for unidirectional composite in the 1–2 plane
ρ	mass density of unidirectional composite
ρ_f	mass density of the fluid
χ_x, χ_θ, $\chi_{x\theta}$	middle surface curvatures and twist curvature
ω	circular frequency
$\mathbf{a}$	vector of nodal displacements
$\ddot{\mathbf{a}}$	vector of nodal accelerations
$\mathbf{A}$	defined by Eq. (25)
$\mathbf{A}_s$	defined by Eq. (28)
$\mathbf{B}$	defined by Eq. (26)
$\mathbf{D}$	defined by Eq. (27)
$\mathbf{F}$	defined by Eq. (32)
$\mathbf{H}$	defined by Eq. (34)
$\mathbf{I}$	defined by Eq. (31)
$\mathbf{I}_5$	5×5 identity matrix
$\mathbf{K}$	stiffness matrix of the shell element
$\mathbf{M}$	mass matrix of the shell element
$\mathbf{M}_f$	defined by Eq. (33)
$\mathbf{N}$	shape function matrix of the shell element
$\mathbf{N}_f$	shape function matrix of the fluid element
$\mathbf{P}$	vector of nodal hydrodynamic pressures
$\boldsymbol{\theta}$	triangular function matrix

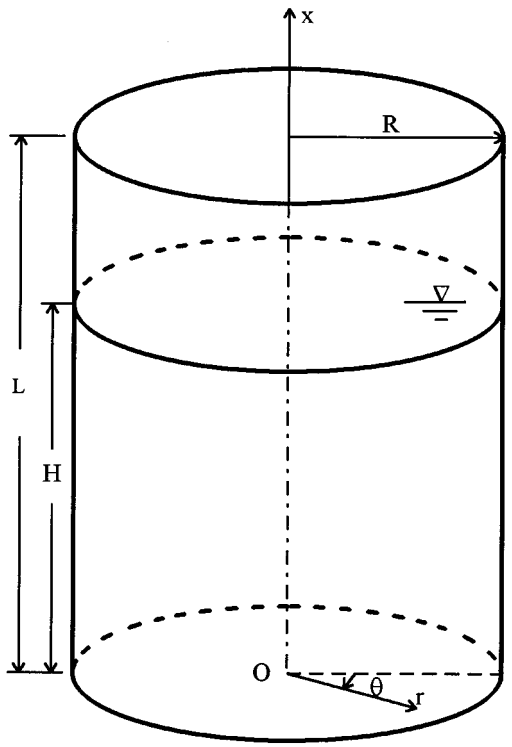

FIG. 1. Geometry of a partially fluid-filled shell and coordinate system of a fluid.

INTRODUCTION

The failure of a partially fluid-filled isotropic circular cylindrical shell due to dynamic loading has received much attention. Advanced composite materials possess high specific strength and stiffness, and super corrosion resistance. The replacement of conventional metal materials by advanced composite materials can improve the bearing capacity of a partially fluid-filled shell. Therefore, in recent years, the use of a partially fluid-filled laminated composite circular cylindrical shell in engineering industry has been steadily increasing. In the design of such a partially fluid-filled composite shell, dynamic response is still a major concern. The free vibration analysis of the partially fluid-filled composite shell is very useful indeed to better study and understand the dynamic behavior.

Owing to the significance of the problem, a few investigators have carried out the vibration analyses of partially fluid-filled laminated composite circular cylindrical shells. On the basis of the first-order shear deformation theory, Jain investigated the vibration of a simply supported fluid-filled circular cylindrical shell composed of multiple isotropic layers using the Rayleigh–Ritz method.[1] Chen and Bert studied the dynamic stability of an orthotropic circular cylindrical shell containing swirling fluid flow using an analytical approach.[2] Based on the first-order shear deformation theory, Chang and Chiou predicted the natural frequency of a fixed–fixed laminated composite circular cylindrical shell conveying a fluid using the Hamilton's principle.[3] Lakis and Laveau discussed the influence of nonlinearity associated with fluid flow on the natural frequency of a circular cylindrical shell partially filled with a fluid.[4] Lakis and Sinno dealt with the axisymmetric and beamlike free vibration problems of an anisotropic circular cylindrical shell partially filled with a liquid.[5] Lakis, Dyke, and Ouriche analyzed the free vibration of an anisotropic fluid-filled conical shell.[6] The semi-analytical methods presented in Refs. 4–6 are based on the Sanders' thin shell theory.

In this paper, free vibrations of partially fluid-filled orthotropic and cross-ply laminated composite circular cylindrical shells are investigated using a semi-analytical procedure based on the Reissner–Mindlin theory and compressible fluid equations. The shell is modeled using unaxisymmetric shear deformable circular cylindrical shell elements. The fluid is modeled using column fluid elements. The equation of motion of the partially fluid-filled shell is derived using the Hamilton's variational principle. Numerical examples are given for the free vibrations of partially fluid-filled orthotropic and cross-ply laminated composite circular cylindrical shells with various boundary conditions. Parametric studies including circumferential wave number, length-to-radius ratio, radius-to-thickness ratio, material property, and boundary condition are carried out. Emphasis is placed on the effects of the fluid filling on the natural frequencies of orthotropic and cross-ply laminated composite circular cylindrical shells.

I. THEORY

Consider a partially fluid-filled cross-ply laminated composite circular cylindrical shell shown in Fig. 1. Here L and R denote the length and the mean radius of the shell, respectively, and H represents the height of the fluid. The laminated shell is presumed to consist of perfectly bonded shell-like laminae. The laminae are linearly elastic. The deflections are small. The Reissner–Mindlin hypothesis is also adopted, that is, normals to the shell middle surface before deformation remain straight but not necessarily normal to the shell middle surface after deformation, and have constant length. Under these assumptions, the generalized strain-displacement relations are given by

$$\begin{Bmatrix} \varepsilon_x \\ \varepsilon_\theta \\ \varepsilon_{x\theta} \end{Bmatrix} = \begin{Bmatrix} \dfrac{\partial u}{\partial x} \\ \dfrac{1}{R}\dfrac{\partial v}{\partial \theta} + \dfrac{w}{R} \\ \dfrac{\partial v}{\partial x} + \dfrac{1}{R}\dfrac{\partial u}{\partial \theta} \end{Bmatrix}, \tag{1}$$

$$\begin{Bmatrix} \chi_x \\ \chi_\theta \\ \chi_{x\theta} \end{Bmatrix} = \begin{Bmatrix} \dfrac{\partial \beta_x}{\partial x} \\ \dfrac{1}{R}\dfrac{\partial \beta_\theta}{\partial \theta} \\ \dfrac{1}{R}\dfrac{\partial \beta_x}{\partial \theta} + \dfrac{\partial \beta_\theta}{\partial x} \end{Bmatrix}, \tag{2}$$

$$\begin{Bmatrix} \gamma_{\theta z} \\ \gamma_{xz} \end{Bmatrix} = \begin{Bmatrix} \dfrac{1}{R}\dfrac{\partial w}{\partial \theta} - \dfrac{v}{R} + \beta_\theta \\ \dfrac{\partial w}{\partial x} + \beta_x \end{Bmatrix}, \tag{3}$$

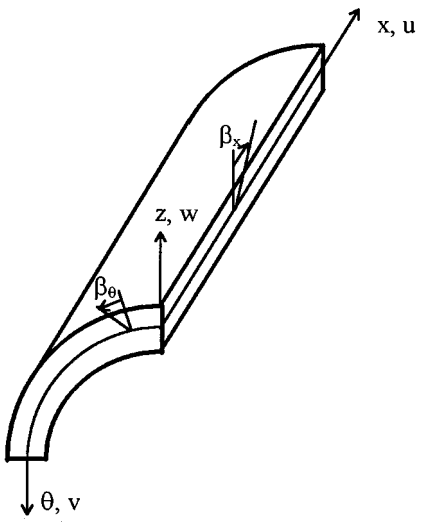

FIG. 2. Sign convention and coordinate system of a shell.

where ε_x, ε_θ, $\varepsilon_{x\theta}$ are the middle surface strains of the shell, χ_x, χ_θ, $\chi_{x\theta}$ are the middle surface curvatures and twist curvature of the shell, $\gamma_{\theta z}, \gamma_{xz}$ are the transverse shear strains of the shell, u, v, and w are the middle surface displacements in the axial, circumferential, and radial directions, respectively, and β_x and β_θ are the rotations of the normal to the middle surface in the x and θ axes, respectively, as is shown in Fig. 2.

The constitutive relations for a cross-ply laminated composite shell are given by[7]

$$\begin{Bmatrix} N_x \\ N_\theta \\ N_{x\theta} \end{Bmatrix} = \begin{bmatrix} A_{11} & A_{12} & 0 \\ A_{12} & A_{22} & 0 \\ 0 & 0 & A_{66} \end{bmatrix} \begin{Bmatrix} \varepsilon_x \\ \varepsilon_\theta \\ \varepsilon_{x\theta} \end{Bmatrix} + \begin{bmatrix} B_{11} & B_{12} & 0 \\ B_{12} & B_{22} & 0 \\ 0 & 0 & B_{66} \end{bmatrix} \begin{Bmatrix} \chi_x \\ \chi_\theta \\ \chi_{x\theta} \end{Bmatrix}, \tag{4}$$

$$\begin{Bmatrix} M_x \\ M_\theta \\ M_{x\theta} \end{Bmatrix} = \begin{bmatrix} B_{11} & B_{12} & 0 \\ B_{12} & B_{22} & 0 \\ 0 & 0 & B_{66} \end{bmatrix} \begin{Bmatrix} \varepsilon_x \\ \varepsilon_\theta \\ \varepsilon_{x\theta} \end{Bmatrix} + \begin{bmatrix} D_{11} & D_{12} & 0 \\ D_{12} & D_{22} & 0 \\ 0 & 0 & D_{66} \end{bmatrix} \begin{Bmatrix} \chi_x \\ \chi_\theta \\ \chi_{x\theta} \end{Bmatrix}, \tag{5}$$

$$\begin{Bmatrix} Q_{\theta z} \\ Q_{xz} \end{Bmatrix} = \begin{bmatrix} A_{44} & 0 \\ 0 & A_{55} \end{bmatrix} \begin{Bmatrix} \gamma_{\theta z} \\ \gamma_{xz} \end{Bmatrix}, \tag{6}$$

where N_x, N_θ, $N_{x\theta}$ are the membrane stress resultants, M_x, M_θ, $M_{x\theta}$ are the moment resultants, and $Q_{\theta z}, Q_{xz}$ are the transverse shear stress resultants. The extensional, extensional-bending coupling, bending, and transverse shear stiffnesses are defined as

$$(A_{ij}, B_{ij}, D_{ij}) = \int_{-h/2}^{h/2} \overline{Q_{ij}}(1, z, z,^2) dz, \quad i,j = 1,2,6, \tag{7}$$

$$A_{ij} = \frac{5}{4} \int_{-h/2}^{h/2} \overline{Q_{ij}} \left(1 - \frac{4z^2}{h^2}\right) dz, \quad i,j = 4,5, \tag{8}$$

where h is the thickness of the shell wall, and the expressions for the reduced stiffness coefficients $\overline{Q_{ij}}$ $(i,j = 1,2,4,5,6)$ in terms of the material properties of the ply are given in Ref. 7.

For irrotational flow of an inviscid fluid undergoing small motions, the hydrodynamic pressure P satisfies the Helmholtz's equation in the r, θ, and x coordinates (see Fig. 1),

$$\frac{\partial^2 P}{\partial r^2} + \frac{1}{r}\frac{\partial P}{\partial r} + \frac{1}{r^2}\frac{\partial^2 P}{\partial \theta^2} + \frac{\partial^2 P}{\partial x^2} - \frac{1}{c^2}\frac{\partial^2 P}{\partial t^2} = 0, \tag{9}$$

where c denotes the speed of sound in the fluid.

When surface gravity waves are considered, on the free surface the pressure P satisfies

$$\frac{\partial P}{\partial x} = -\frac{1}{g}\frac{\partial^2 P}{\partial t^2}, \tag{10}$$

where g is the gravity acceleration.

On the interface between the fluid and the shell the pressure P satisfies

$$\frac{\partial P}{\partial \overline{n}} = -\rho_f \frac{\partial^2 w}{\partial t^2}, \tag{11}$$

where $\overline{n}$ is the unit normal to the wetted surface of the shell and ρ_f is the mass density of the fluid.

The Hamilton variational principle is used to derive the equation of motion of a partially fluid-filled shell. The Hamilton variational principle for the free vibration of a partially fluid-filled laminated composite circular cylindrical shell is given by

$$\delta \int_{t_0}^{t_1} (U - T + J) dt = 0, \tag{12}$$

where the times t_1 and t_0 are arbitrary, U and T are the potential energy and kinetic energy of the shell, respectively, and J is the energy stored in the fluid.

The two-node straight axisymmetric circular cylindrical shell element presented by Zienkiewicz *et al.*[8] is extended here to the unaxisymmetric case in order to consider the coupling between in-plane and transverse variables. For free vibration, the displacement field within an element for circumferential wave number n may be expressed as

$$[u \quad v \quad w \quad \beta_x \quad \beta_\theta]^T = \boldsymbol{\theta}\,\mathbf{N}\mathbf{a}, \tag{13}$$

where the triangular function matrix $\boldsymbol{\theta}$, the shape function matrix $\mathbf{N}$ of the shell element, and the nodal displacement vector $\mathbf{a}$ of the shell element are respectively given by

$$\theta = \begin{bmatrix} \cos n\theta & 0 & 0 & 0 & 0 \\ 0 & \sin n\theta & 0 & 0 & 0 \\ 0 & 0 & \cos n\theta & 0 & 0 \\ 0 & 0 & 0 & \cos n\theta & 0 \\ 0 & 0 & 0 & 0 & \sin n\theta \end{bmatrix}, \tag{14}$$

$$\mathbf{N} = [N_i \mathbf{I}_5 \quad N_j \mathbf{I}_5], \tag{15}$$

$$\mathbf{a}=[u_i \quad v_i \quad w_i \quad \beta_{xi} \quad \beta_{\theta i} \quad u_j \quad v_j \quad w_j \quad \beta_{xj} \quad \beta_{\theta j}]^T. \tag{16}$$

In Eq. (15) $\mathbf{I}_5$ is the 5×5 identity matrix, and the shape functions N_i and N_j of the shell element are defined as $N_i=1-\eta$ and $N_j=\eta$ with $\eta=x/l$, where l is the length of the element and subscripts i and j denote the front and rear ends of the shell element, respectively.

When the shell element is filled with a fluid, the potential energy U is given by

$$U=\frac{1}{2}\int_0^{2\pi}\int_0^1\left(\begin{Bmatrix}\varepsilon_x\\ \varepsilon_\theta\\ \varepsilon_{x\theta}\end{Bmatrix}^T\begin{Bmatrix}N_x\\ N_\theta\\ N_{x\theta}\end{Bmatrix}+\begin{Bmatrix}\chi_x\\ \chi_\theta\\ \chi_{x\theta}\end{Bmatrix}^T\begin{Bmatrix}M_x\\ M_\theta\\ M_{x\theta}\end{Bmatrix}+\begin{Bmatrix}\gamma_{\theta z}\\ \gamma_{xz}\end{Bmatrix}^T\begin{Bmatrix}Q_{\theta z}\\ Q_{xz}\end{Bmatrix}\right)Rl\,d\eta\,d\theta-\int_0^{2\pi}\int_0^1 wPRl\,d\eta\,d\theta, \tag{17}$$

where P is the hydrodynamic pressure acting on the wall of the shell. The kinetic energy of the shell element T can be expressed as

$$T=\frac{1}{2}\int_0^{2\pi}\int_0^1\int_{-h/2}^{h/2}\rho[\dot{u}^2+\dot{v}^2+\dot{w}^2+z^2(\dot{\beta}_x^2+\dot{\beta}_\theta^2)]Rl\,dz\,d\eta\,d\theta, \tag{18}$$

where ρ is the mass density of the shell and $\dot{u}$, $\dot{v}$, $\dot{w}$ are the middle surface velocities in the axial, circumferential, and radial directions, respectively.

The column fluid element presented by Cao and Cheung[9] is employed to model the fluid. When the effect of fluid sloshing is neglected, the hydrodynamic pressure P within an element for circumferential wave number n may be expressed as

$$P=\mathbf{N}_f\mathbf{p}\cos n\theta, \tag{19}$$

where the shape function matrix $\mathbf{N}_f$ of the fluid element and the vector $\mathbf{p}$ of nodal hydrodynamic pressures are respectively given by

$$\mathbf{N}_f=[N_i\zeta \quad N_i\zeta^2 \quad N_i\zeta^3 \quad N_i\zeta^4 \quad N_j\zeta \quad N_j\zeta^2 \quad N_j\zeta^3 \quad N_j\zeta^4], \tag{20}$$

$$\mathbf{p}=[p_{1i} \quad p_{2i} \quad p_{3i} \quad p_{4i} \quad p_{1j} \quad p_{2j} \quad p_{3j} \quad p_{4j}]^T. \tag{21}$$

In Eq. (20) $\zeta=r/R$. The energy stored in the fluid element is given by

$$J=\int_0^{2\pi}\int_0^1\int_0^1\left\{\frac{1}{2}\left[\left(\frac{\partial P}{R\partial\zeta}\right)^2+\left(\frac{\partial P}{R\zeta\partial\theta}\right)^2+\left(\frac{\partial P}{l\partial\eta}\right)^2\right]+\frac{P}{c^2}\frac{\partial^2 P}{\partial t^2}\right\}R^2 l\zeta\,d\zeta\,d\eta\,d\theta+\int_0^{2\pi}\int_0^1\frac{P}{g}\frac{\partial^2 P}{\partial t^2}\times R^2\zeta\,d\zeta\,d\theta+\int_0^{2\pi}\int_0^1\frac{\partial^2 w}{\partial t^2}\rho_f PRl\,d\eta\,d\theta. \tag{22}$$

Substituting Eqs. (17), (18), and (22) into Eq. (12), performing variational operations, and using the orthogonal property of the trigonometric functions give the equation of motion of the partially fluid-filled shell,

$$\begin{bmatrix}\mathbf{M} & \mathbf{0}\\ \rho_f\mathbf{F}^T & \mathbf{M}_f\end{bmatrix}\begin{Bmatrix}\ddot{\mathbf{a}}\\ \ddot{\mathbf{p}}\end{Bmatrix}+\begin{bmatrix}\mathbf{K} & -\mathbf{F}\\ \mathbf{0} & \mathbf{H}\end{bmatrix}\begin{Bmatrix}\mathbf{a}\\ \mathbf{p}\end{Bmatrix}=\mathbf{0}, \tag{23}$$

where the stiffness matrix $\mathbf{K}$ of the shell element is given by

$$\mathbf{K}=\int_0^1[\mathbf{B}_m^T\mathbf{A}\mathbf{B}_m+\mathbf{B}_m^T(\mathbf{B}+\mathbf{B}^T)\mathbf{B}_b+\mathbf{B}_b^T\mathbf{D}\mathbf{B}_b+\mathbf{B}_s^T\mathbf{A}_s\mathbf{B}_s]Rl\,d\eta. \tag{24}$$

In Eq. (24) the strain-displacement matrices $\mathbf{B}_m=[\mathbf{B}_{mi} \quad \mathbf{B}_{mj}]$, $\mathbf{B}_b=[\mathbf{B}_{bi} \quad \mathbf{B}_{bj}]$, and $\mathbf{B}_s=[\mathbf{B}_{sl} \quad \mathbf{B}_{sj}]$ are shown in Ref. 10, and

$$\mathbf{A}=\begin{bmatrix}A_{11}\delta_1 & A_{12}\delta_1 & 0\\ A_{12}\delta_1 & A_{22}\delta_1 & 0\\ 0 & 0 & A_{66}\delta_2\end{bmatrix}, \tag{25}$$

$$\mathbf{B}=\begin{bmatrix}B_{11}\delta_1 & B_{12}\delta_1 & 0\\ B_{12}\delta_1 & B_{22}\delta_1 & 0\\ 0 & 0 & B_{66}\delta_2\end{bmatrix}, \tag{26}$$

$$\mathbf{D}=\begin{bmatrix}D_{11}\delta_1 & D_{12}\delta_1 & 0\\ D_{12}\delta_1 & D_{22}\delta_1 & 0\\ 0 & 0 & D_{66}\delta_2\end{bmatrix}, \tag{27}$$

$$\mathbf{A}_s=\begin{bmatrix}A_{44}\delta_2 & 0\\ 0 & A_{55}\delta_1\end{bmatrix}, \tag{28}$$

where

$$\delta_1=\begin{cases}2\pi, & n=0,\\ \pi, & n\neq 0,\end{cases}\qquad \delta_2=\begin{cases}0, & n=0,\\ \pi, & n\neq 0.\end{cases} \tag{29}$$

In Eq. (23) the mass matrix $\mathbf{M}$ of the shell element is given by

$$\mathbf{M}=\int_0^1\mathbf{N}^T\,\mathbf{I}\mathbf{N}Rl\,d\eta, \tag{30}$$

where

$$\mathbf{I}=\int_{-h/2}^{h/2}\begin{bmatrix}\delta_1\rho & 0 & 0 & 0 & 0\\ 0 & \delta_2\rho & 0 & 0 & 0\\ 0 & 0 & \delta_1\rho & 0 & 0\\ 0 & 0 & 0 & \delta_1\rho z^2 & 0\\ 0 & 0 & 0 & 0 & \delta_2\rho z^2\end{bmatrix}dz. \tag{31}$$

In Eq. (23) the coupling term $\mathbf{F}$ due to the hydrodynamic pressure is given by

$$\mathbf{F}=\delta_1\int_0^1\mathbf{N}^T\mathbf{n}^T\mathbf{N}_f|_{\zeta=1}Rl\,d\eta, \tag{32}$$

where $\mathbf{n}=[0 \quad 0 \quad 1 \quad 0 \quad 0]$.

In Eq. (23) $\mathbf{M}_f$ and $\mathbf{H}$ are respectively given by

TABLE I. Natural frequency (in Hz) of a clamped–free (0°/90°) laminated composite circular cylindrical shell.[a]

		Number of elements used				
n	m	7	14	21	28	32
1	1	640	641	642	642	642
11	1	565	670	704	705	705

[a]$L/R=2$, $R/h=200$.

$$\mathbf{M}_f=\frac{\delta_1}{c^2}\int_0^1\int_0^1 \mathbf{N}_f^T\mathbf{N}_f R^2 l\zeta\, d\zeta\, d\eta + \frac{\delta_1}{g}\int_0^1 (\mathbf{N}_f^T\mathbf{N}_f)|_{\eta=1} R^2\zeta\, d\zeta, \tag{33}$$

$$\mathbf{H}=\int_0^1\int_0^1\left[\delta_1\left(\frac{\partial\mathbf{N}_f^T}{R\partial\zeta}\right)\left(\frac{\partial\mathbf{N}_f}{R\partial\zeta}\right)+n^2\delta_2\left(\frac{\mathbf{N}_f^T}{R\zeta}\right)\left(\frac{\mathbf{N}_f}{R\zeta}\right) + \delta_1\left(\frac{\partial\mathbf{N}_f^T}{l\partial\eta}\right)\left(\frac{\partial\mathbf{N}_f}{l\partial\eta}\right)\right]R^2 l\zeta\, d\eta\, d\zeta. \tag{34}$$

Putting $\mathbf{a}=\overline{\mathbf{a}}\cos\omega t$ and $\mathbf{p}=\overline{\mathbf{p}}\cos\omega t$ and inserting them into Eq. (23) give the characteristic equation of the partially fluid-filled shell

$$\left|\begin{bmatrix}\mathbf{K} & -\mathbf{F}\\ \mathbf{0} & \mathbf{H}\end{bmatrix}-\omega^2\begin{bmatrix}\mathbf{M} & \mathbf{0}\\ \rho_f\mathbf{F}^T & \mathbf{M}_f\end{bmatrix}\right|=0, \tag{35}$$

where ω is the circular frequency of the partially fluid-filled shell.

II. NUMERICAL RESULTS AND DISCUSSION

In this section, the influence of the fluid filling on the natural frequencies of orthotropic and cross-ply laminated composite circular cylindrical shells is studied numerically using the foregoing theory. A lamina numbering increases from the outer to the inner shell surface. The 0 ° and 90 ° layers have all-axial and all-circumferential fiber orientations, respectively. An orthotropic shell is composed of 0 ° layers only. The lamina material properties used are[11] $E_1=206.9$ GPa, $E_2=18.62$ GPa, $G_{12}=4.48$ GPa, $G_{13}=G_{12}$, $G_{23}=0.5G_{12}$, $\nu_{12}=0.28$, and $\rho=2048$ kg m^{-3}. The fluid is taken as water with the mass density, ρ_f, of 1000 kg m^{-3}.

A convergence study is made to find the number of elements required for the analyses. Table I shows the natural frequency of a clamped–free (0 °/90 °) laminated composite circular cylindrical shell. The clamped boundary condition implies $u=v=w=\beta_x=\beta_\theta=0$, while at the free end all the nodal degrees of freedom are unconstrained. It can be seen that with 28 elements, the frequencies are converged to a very good degree of accuracy. In the subsequent calculations, the shell is divided axially into 28 elements. The length of the fluid element is the same as that of the shell element.

First, three examples are used to clarify the validity of the present analysis. The first two examples are for simply supported orthotropic and cross-ply laminated composite circular cylindrical shells. The simply supported boundary condition implies that at one end the boundary conditions are $u=w=\beta_\theta=0$, whereas at the other end the boundary conditions are $w=\beta_\theta=0$. The natural frequencies are shown in Fig. 3 and compared with those given by Sheinman and Weissman.[11] These results are obtained for longitudinal mode $m=1$. Good agreement is achieved.

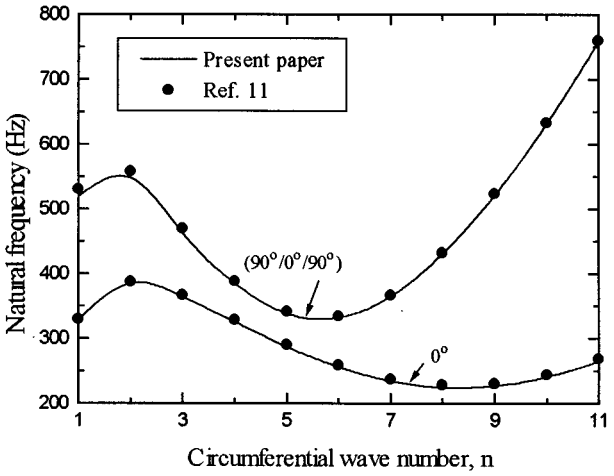

FIG. 3. Natural frequencies of simply supported laminated composite circular cylindrical shells ($L=0.381$ m, $R=0.1905$ m, $h=0.501\times10^{-3}$ m, $m=1$).

The third example is for a clamped–free thin circular cylindrical shell partially filled with a fluid. The natural frequency is shown in Fig. 4 and compared with the experimental results provided by Chiba, Yamaki, and Tani.[12] These results are obtained for circumferential wave number $n=5$ and longitudinal mode $m=1$. The agreement between the present and experimental results is very good.

Now natural frequencies of partially fluid-filled orthotropic and cross-ply laminated composite circular cylindrical shells with various boundary conditions are calculated.

Figures 5 and 6 show the variations of the natural frequencies with circumferential wave number for clamped–free orthotropic and (0 °/90 °) laminated composite circular cylindrical shells partially filled with a fluid, respectively. For the sake of comparison, the natural frequencies of the corresponding empty shells are also plotted in these figures. As can be seen from these figures, the fluid filling can reduce significantly the magnitude of the natural frequencies of the shells. This phenomenon may be explained intuitively. For a partially fluid-filled shell, the fluid filling increases the total mass of the shell, hence the natural frequencies of the shell decrease. In addition, from Figs. 5 and 6 it can also be seen that the variations of the natural frequencies with circumferential wave number for partially fluid-filled orthotropic and cross-ply laminated composite circular cylindrical shells are similar to those for the corresponding empty shells. For these numerical examples, the natural frequencies of both partially fluid-filled and empty shells first decrease to a minimum and then increase with circumferential wave number. The fluid filling cannot shift the lowest natural frequencies of these shells. This indicates that the fluid filling has negligible effect on the distribution of the natural frequencies of the shells.

Figures 7 and 8 show the effect of the fluid filling on the

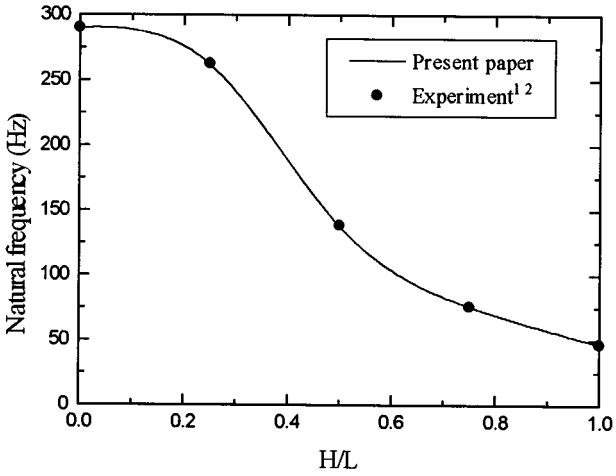

FIG. 4. Natural frequency of a clamped–free isotropic circular cylindrical shell partially filled with a fluid ($R=0.1$ m, $L=0.1139$ m, $h=0.247\times10^{-3}$ m, $E=5.56$ GPa, $\nu=0.3$, $\rho=1405$ kg m^{-3}, $n=5$, $m=1$).

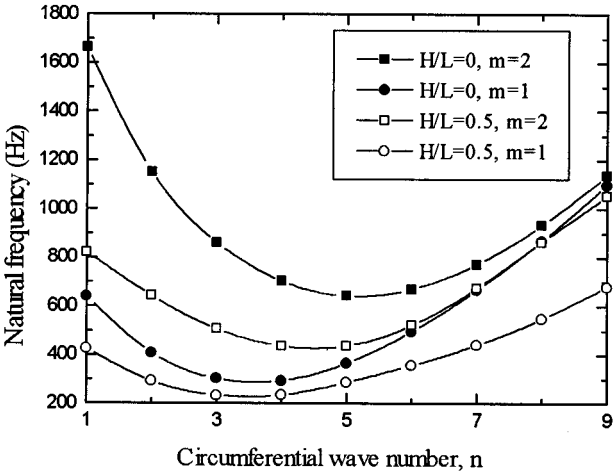

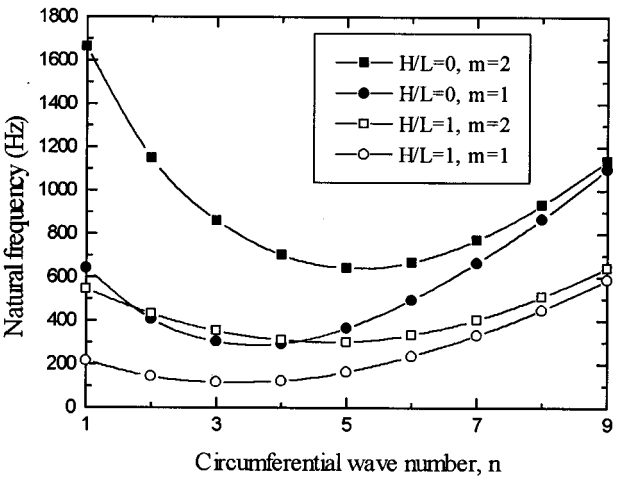

FIG. 5. Natural frequency of a clamped–free orthotropic circular cylindrical shell partially filled with a fluid ($L/R=2$, $R/h=50$).

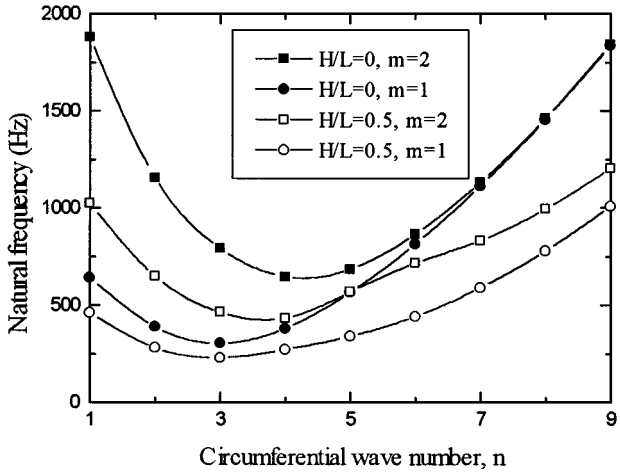

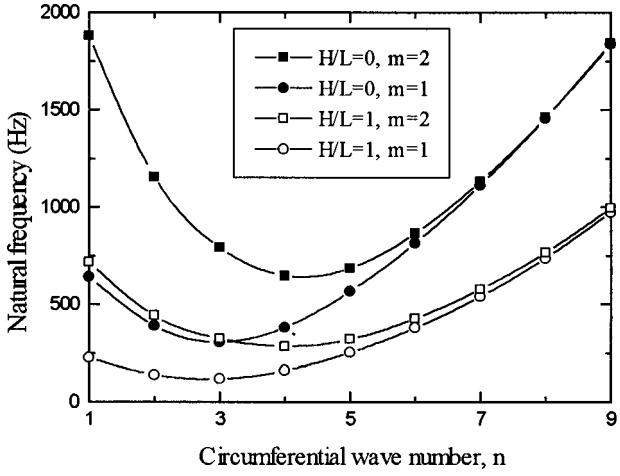

FIG. 6. Natural frequency of a clamped–free (0°/90°) laminated composite circular cylindrical shell partially filled with a fluid ($L/R=2$, $R/h=50$).

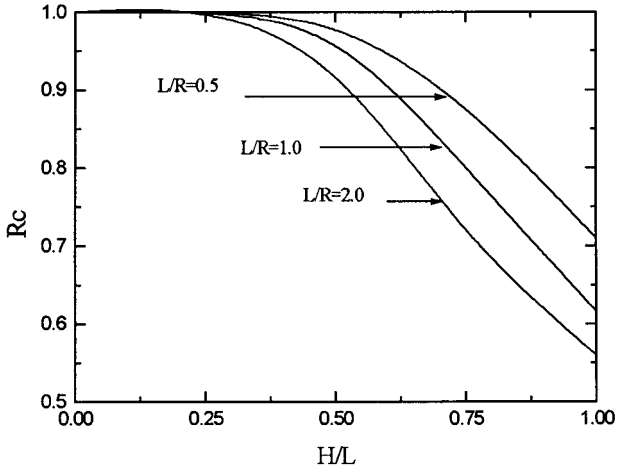

FIG. 7. Effect of the fluid filling on the fundamental natural frequencies of clamped–free orthotropic circular cylindrical shells with different length to radius ratios ($R/h=20$).

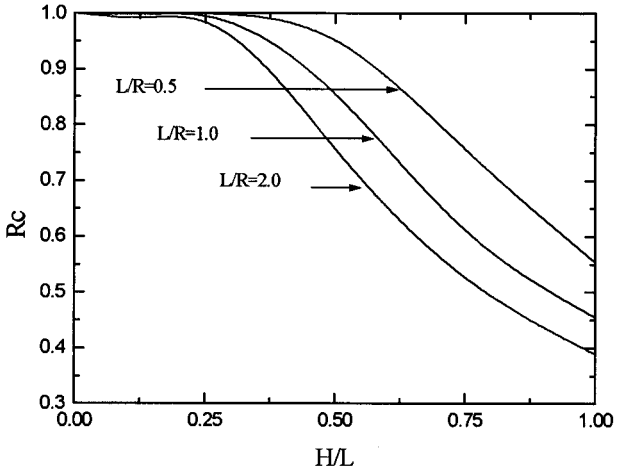

FIG. 8. Effect of the fluid filling on the fundamental natural frequencies of clamped–free (0°/90°) laminated composite circular cylindrical shells with different length to radius ratios ($R/h=50$).

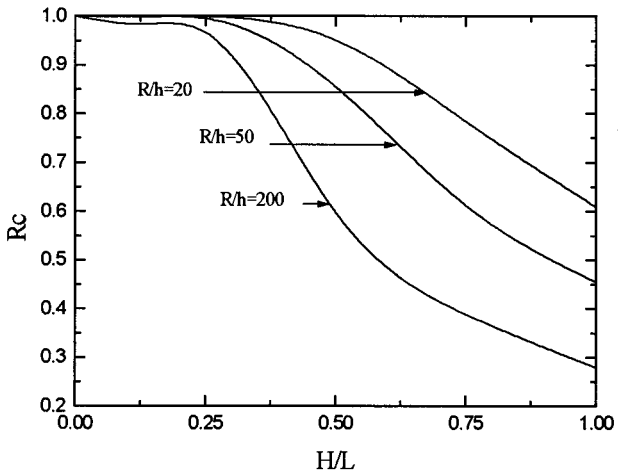

FIG. 10. Effect of the fluid filling on the fundamental natural frequencies of clamped–free (0°/90°) laminated composite circular cylindrical shells with different radius to thickness ratios ($L/R=1$).

fundamental natural frequencies of clamped-free orthotropic and (0 °/90 °) laminated composite circular cylindrical shells with different length to radius ratios, respectively. The fundamental natural frequency ratio Rc is defined as the ratio of the natural frequency of the partially fluid-filled shell to that of the corresponding empty shell. The curves in these figures reveal that the influence of the fluid filling on the natural frequencies of the shells becomes strong with the length to radius ratio. The behavior is due to the change in the stiffness of the shell. As the ratio of length to radius increases, the shell becomes flexible. Accordingly, the shell is sensitive to the fluid filling.

In addition, from Figs. 7 and 8 it can be seen more clearly how the reduction of the natural frequencies of the shells varies with the height of the fluid filling. For these numerical examples, as the height of the fluid filling increases, the natural frequencies of the shells decrease first slightly and then quickly.

Figures 9 and 10 show the effect of the fluid filling on the fundamental natural frequencies of clamped–free orthotropic and (0 °/90 °) laminated composite circular cylindrical shells with different radius to thickness ratios, respectively. It is obvious that the influence of the fluid filling on the natural frequencies of the shells becomes strong as the ratio of radius to thickness increases. This behavior may be explained from the change of the stiffness of the shell. As the ratio of radius to thickness increases, the stiffness of the shell reduces. As a result, the reduction of the natural frequency of the shell becomes large.

Besides, it can also be seen from Figs. 9 and 10 that as the height of the fluid filling increases, the pattern of the variation of the natural frequency of a thinner shell is different from that of a thicker shell. For example, for $H/L>0$, the natural frequencies of the shells with $R/h=200$ begin to reduce, while for $H/L>0.25$, the natural frequencies of the shells with $R/h=20$ and 50 begin to decrease.

Figures 11 and 12 show the effect of the fluid filling on

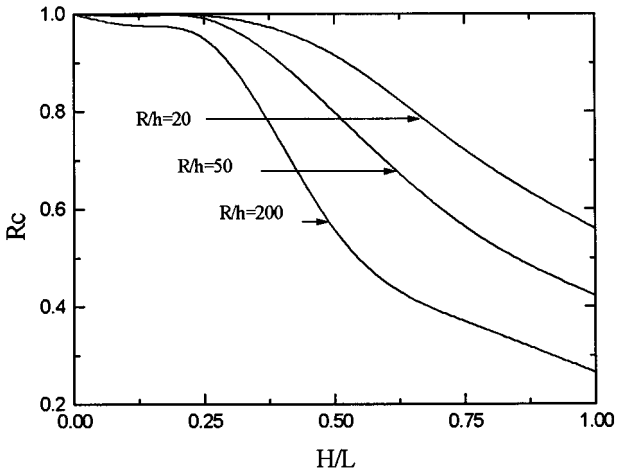

FIG. 9. Effect of the fluid filling on the fundamental natural frequencies of clamped–free orthotropic circular cylindrical shells with different radius thickness ratios ($L/R=2$).

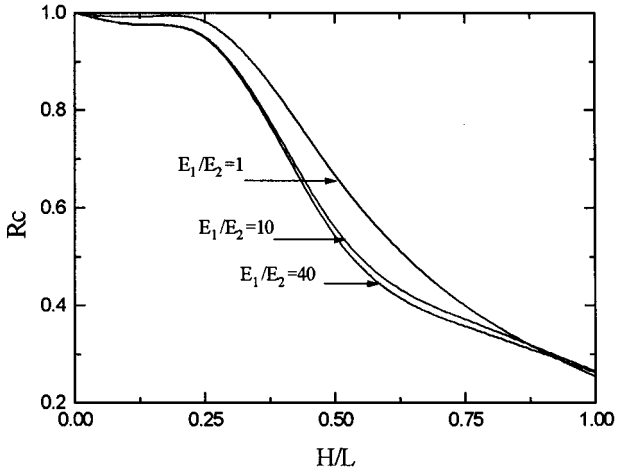

FIG. 11. Effect of the fluid filling on the fundamental natural frequencies of clamped–free orthotropic circular cylindrical shells with different material properties ($G_{12}/E_2=0.24$, $\nu_{12}=0.28$, $G_{13}=G_{12}$, $G_{23}=0.5G_{12}$, $L/R=2$, $R/h=200$).

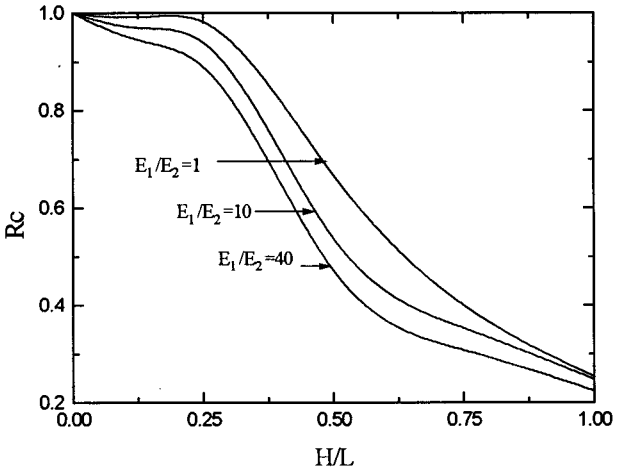

FIG. 12. Effect of the fluid filling on the fundamental natural frequencies of clamped–free (0°/90°) laminated composite circular cylindrical shells with different material properties ($G_{12}/E_2=0.24$, $\nu_{12}=0.28$, $G_{13}=G_{12}$, $G_{23}=0.5G_{12}$, $L/R=2$, $R/h=200$).

the fundamental natural frequencies of clamped-free orthotropic and (0°/90°) laminated composite circular cylindrical shells with different material properties, respectively. Clearly, the influence of the fluid filling on the natural frequencies of the shells becomes strong as E_1/E_2 increases. Comparison of two figures shows that as E_1/E_2 increases, the reduction of the natural frequencies of the orthotropic shell is different from that of the cross-ply shell. As can be seen from Fig. 11, the reduction of the natural frequencies of the orthotropic shell is remarkable when E_1/E_2 increases from 1 to 10. When E_1/E_2 continues to increase, the natural frequencies reduce only slightly. However, the results in Fig. 12 indicate that the reduction of the natural frequencies of the cross-ply shell is remarkable all the way as E_1/E_2 increases.

Figures 13 and 14 show the effect of the fluid filling on the fundamental natural frequencies of orthotropic and (0°/90°) laminated composite circular cylindrical shells with different boundary conditions, respectively. At two simply supported ends the boundary conditions imply $w=\beta_\theta=0$. From these figures it can be found that the fluid filling has more considerable influence on the natural frequencies of the simply supported and clamped–clamped shells than on those of the clamped–free shell. This shows that relaxing one end constraint can reduce the effect of the fluid filling on the natural frequencies of the shells. Besides, the natural frequencies of the simply supported shells are different from those of the clamped–clamped shells. For $H/L\leqslant 0.5$, the reduction of the natural frequencies of the simply supported shells due to the fluid filling is more remarkable than that for the clamped–clamped shells. It can be seen that the simply supported shells are more sensitive to the fluid filling than the clamped–clamped shells when the shells become half-full from empty. For $H/L>0.5$, the reductions of the natural frequencies of the simply supported and clamped–clamped shells due to the fluid filling are almost identical. In other words, the influences of the fluid filling on the natural frequencies of the simply supported and clamped–clamped shells are almost the same when the shells become full from half-full.

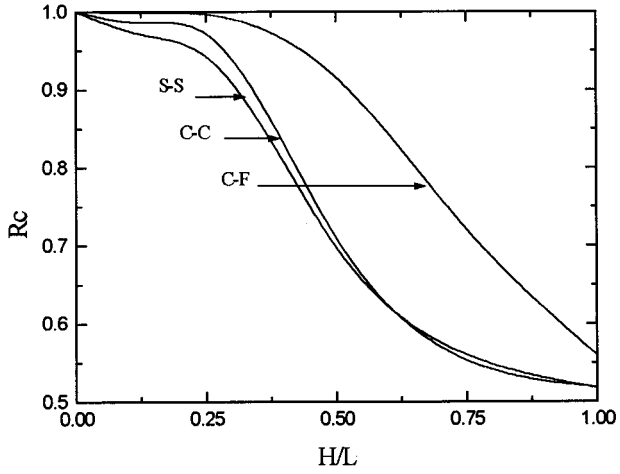

FIG. 13. Effect of the fluid filling on the fundamental natural frequencies of orthotropic circular cylindrical shells with different boundary conditions ($L/R=2$, $R/h=20$).

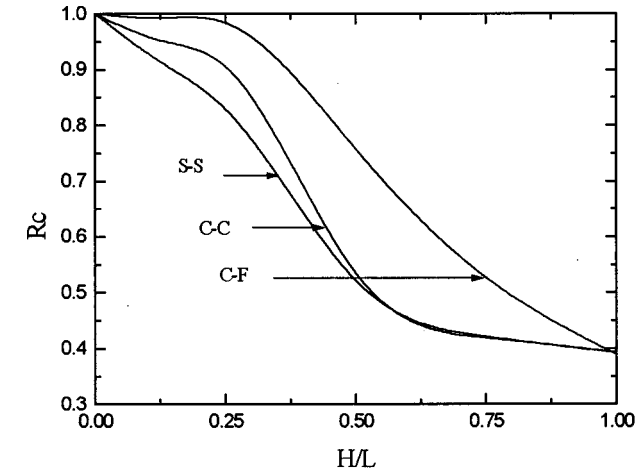

FIG. 14. Effect of the fluid filling on the fundamental natural frequencies of (0°/90°) laminated composite circular cylindrical shells with different boundary conditions ($L/R=2$, $R/h=50$).

III. CONCLUSIONS

Free vibrations of partially fluid-filled orthotropic and cross-ply laminated composite circular cylindrical shells with various boundary conditions are studied using a semi-analytical method based on the Reissner–Mindlin shell theory and compressible fluid equations. Based on the numerical results presented in this paper, the following conclusions may be drawn:

(a) The fluid filling can reduce significantly the natural frequencies of orthotropic and cross-ply laminated composite circular cylindrical shells, but it has negligible effect on the distribution of the natural frequencies of these shells.
(b) As the ratio of length to radius increases, the effect of

the fluid filling on the natural frequencies of orthotropic and cross-ply laminated composite circular cylindrical shells becomes strong.

(c) The influence of the fluid filling on the natural frequencies of orthotropic and cross-ply laminated composite circular cylindrical shells increases with the ratio of radius to thickness.

(d) The influence of the fluid filling on the natural frequencies of orthotropic and cross-ply laminated composite circular cylindrical shells increases as E_1/E_2 increases.

(e) When the other parameters are the same, the fluid filling has more considerable effect on the natural frequencies of orthotropic and cross-ply laminated composite circular cylindrical shells with simply supported and clamped–clamped boundary conditions than on those of the corresponding clamped–free shells.

ACKNOWLEDGMENTS

The authors are grateful to the Research Committee of The Hong Kong Polytechnic University for the support of this investigation. The authors would like to thank Professor G. Lin of Dalian University of Technology, China, for the helpful discussions.

[1] R. K. Jain, ''Vibration of fluid-filled, orthotropic cylindrical shells,'' J. Sound Vib. **37**, 379–388 (1974).

[2] T. L. C. Chen and C. W. Bert, ''Dynamic stability of isotropic or composite material cylindrical shells containing swirling fluid flow,'' J. Appl. Mech. **44**, 112–116 (1977).

[3] J. S. Chang and W. J. Chiou, ''Natural frequencies and critical velocities of fixed-fixed laminated circular cylindrical shells conveying fluids,'' Comput. Struct. **57**, 929–939 (1995).

[4] A. A. Lakis and A. Laveau, ''Non-linear dynamic analysis of anisotropic cylindrical shells containing a flowing fluid,'' Int. J. Solids Struct. **28**, 1079–1094 (1991).

[5] A. A. Lakis and M. Sinno, ''Free vibration of axisymmetric and beam-like cylindrical shells partially filled with liquid,'' Int. J. Num. Meth. Eng. **33**, 235–268 (1992).

[6] A. A. Lakis, P. V. Dyke, and H. Ouriche, ''Dynamic analysis of anisotropic fluid-filled conical shells,'' J. Fluids Struct. **6**, 135–162 (1992).

[7] S. W. Tsai and H. T. Hahn, *Introduction to Composite Materials* (Technomic, Westport, CT, 1980).

[8] O. C. Zienkiewicz, J. Bauer, K. Morgan, and E. Onate, ''A simple and efficient element for axisymmetric shells,'' Int. J. Num. Meth. Eng. **11**, 1545–1558 (1977).

[9] Z. Y. Cao and Y. K. Cheung, ''A semi-analytical method for structure-internal liquid interaction problems,'' Appl. Math. Mech. **6**, 1–8 (1985) (in Chinese).

[10] Z. C. Xi, L. H. Yam, and T. P. Leung, ''Semi-analytical study of free vibration of composite shells of revolution based on the Reissner–Mindlin assumption,'' Int. J. Solids Struct. **33**, 851–863 (1996).

[11] I. Sheinman and S. Weissman, ''Coupling between symmetric and anti-symmetric modes in shells of revolution,'' J. Compos. Mater. **21**, 988–1007 (1987).

[12] M. Chiba, N. Yamaki, and J. Tani, ''Free vibration of a clamped-free circular cylindrical shell partially filled with liquid—part 3: Experimental analysis,'' Thin-Walled Struct. **3**, 1–14 (1985).